Heliyon 8 (2022) e09030

Contents lists available at ScienceDirect

Heliyon

journal homepage: www.cell.com/heliyon

Research article

Study of valproic acid liposomes for delivery into the brain through an intranasal route

Mahdi Jufri [a,*], Alhara Yuwanda [a], Silvia Surini [a], Yahdiana Harahap [b]

[a] Laboratory of Pharmaceutical Technology, Faculty of Pharmacy, University of Indonesia, Depok, 16424, Indonesia
[b] Laboratory of Bio Availability/Bio Equivalence (BA/BE), Faculty of Pharmacy, University of Indonesia, Depok, 16424, Indonesia

ARTICLE INFO

Keywords:
Intranasal
Liposome
Valproic acid
Penetration
Epilepsy
Brain

ABSTRACT

Intranasal drug transport through the olfactory route to the brain is an effective drug route for increased absorption and bioavailability of the drug. The objective of this study was to increase the penetration of valproic acid as an anticonvulsant into a delivery system comprising liposomes. Valproic acid liposomes were prepared by a thin-layer hydration technique using soybean phosphatidylcholine and cholesterol as the main ingredients. The formulations were evaluated for diameter size, entrapment efficiency (EE), zeta potential, polydispersity index, and morphology. *ex vivo* permeation using sheep nasal mucosa and in vivo efficacy were assessed by performing a pharmacokinetic study in Wistar albino rats following intranasal administration of the formulations in comparison with pure drug. The mean size particle of optimized liposomes ranged from 90 to 210 nm with a low polydispersity index (<0.5). The EE of optimized liposomes was between 60% and 85%, increasing the concentration of phosphatidylcholine added to the formula. Transmission electron microscopy observations (40,000×) showed that valproic acid liposomes have a spherical molecular shape and a particle size of below 250 nm. The ex vivo and in vivo results showed that liposomal formulations provided enhanced brain exposure. Among the formulations studied, Formula 4 (F4) showed greater uptake of valproic acid into the brain than plasma. The high brain targeting efficiency index for F4 indicated the preferential transport of the drug to the brain. The study demonstrated the successful formulation of surface-modified valproic acid liposomes for nasal delivery with brain targeting potential.

1. Introduction

Research on the method for increasing drug delivery efficiency to the brain is fascinating. In addition to modifying drug compounds, many attempts have been made to alter dosage forms and drug delivery systems. One of the routes for drug delivery is intranasal administration [1]. Intranasal administration has been used as an alternative route as this shows potential for rapid systemic drug absorption into the brain [2,3]. The nasal cavity transports drugs directly to the brain through olfactory neurons or the trigeminal nerve, and drugs are absorbed via the nasal mucosa. The brain has two natural barriers to drug absorption: the blood–cerebrospinal fluid barrier (BCSFB) and the blood–brain barrier (BBB) [4, 5, 6]. The clearance mechanism reduces the retention time of the drug in the nasal cavity and the time for absorption [7]. Nasal mucociliary clearance results in decreased drug absorption, so a strategy is needed to increase the absorption of drugs [8], especially drugs that target the central nervous system (CNS) [9, 10, 11].

Valproic acid (VPA) is an effective drug to prevent grand mal epilepsy with tonic–clonic seizures. VPA has a molecular weight of 144 g/mol and is lipophilic (log P = 2.54). VPA preparations are currently in the form of oral and intravenous injections. Previous studies reported that the distribution and bioavailability of VPA in the brain are relatively low compared with other epilepsy drugs, such as phenytoin or phenobarbital, via the oral route. The bioavailability of VPA is very low because it is rapidly metabolized through the first-cross metabolism, which is then conjugated by glucuronidation, sulfation, or methylation reactions [12]. Compounds measured in high levels in plasma are not VPA compounds but are metabolites that are active because more than 90% of the drugs are eliminated via the first-cross metabolism. Another factor that causes low bioavailability of drugs is the efflux pump mechanism in P-glycoprotein in brain microvessel endothelial cells. Based on the results found in the index of efflux studies in the brain, it was found that the efflux clearance of VPA on the BBB was 2.7 times greater than the influx clearance of drugs tested in vivo [13].

* Corresponding author.
E-mail address: mahdi.jufri@farmasi.ui.ac.id (M. Jufri).

https://doi.org/10.1016/j.heliyon.2022.e09030
Received 20 August 2021; Received in revised form 15 November 2021; Accepted 24 February 2022

One solution to overcome the problem of low oral bioavailability in VPA is to administer the drug via another route, i.e., intranasal. The intranasal route is one of the most effective pathways for delivering drugs directly to the brain via olfactory neurons and trigeminal pathways. Drug delivery to the brain is the process of passing CNS through the BBB and the BCSFB. The intranasal route and being effective for drug delivery to the brain can also increase patient comfort. Based on literature studies, in vivo research has examined about 35–40 drug compounds with brain target organs administered via the intranasal route. These studies have been successfully distributed to experimental animals such as carbamazepine, dopamine, neurotoxic metals, local anesthetics, carboxylic acids, and nerve growth factors. VPA using intranasal pathways in the nanostructured lipid carrier (NLC) system shows an increase in the ratio of drug concentrations in the brain compared with blood plasma [14]. Liposomes are potential drug delivery candidates and are effective in penetrating through the BBB. To increase the penetration of VPA, medicinal ingredients are incorporated into nanocarrier systems, such as NLCs [14], dendrimers [15], nanotubes [16], nanoemulsions [17], and liposomes [18]. Liposomes are an effective delivery system to enhance drug penetration into the brain. Liposome delivery systems are phosphatidylcholine- and cholesterol-based carrier systems. These carriers have structural characteristics resembling physiological membranes of the body so that their biocompatibility is higher than that of other carrier systems such as microemulsions and NLCs [19]. In this study, a new formulation of VPA liposomes for intranasal administration was developed. Characterization of physical properties, such as particle size, morphology, zeta potential, pH, and stability, was carried out on VPA liposome preparations. Ex vivo diffusion studies were also performed using the sheep nasal mucous membrane. An in vivo study using Wistar albino rats was conducted to evaluate the pharmacokinetic profile and drug biodistribution. Drug levels of VPA liposomes were compared with pure drugs in blood plasma and the brain.

2. Materials and methods

2.1. Materials

Phospholipon® 90 H and cholesterol products were obtained from Shanghai Soyoung Biotech. Inc. (Shanghai, China). The VPA reference standard was provided by Octagon Chemical Limited (Yantai, China). Sartorius membrane D0405-100FT dialysis tubing was provided by Sigma-Aldrich (St. Louis, USA). Disodium hydrogen phosphate, potassium dihydrogen phosphate, sodium chloride, potassium chloride, acetonitrile, methanol, glacial acetic acid, and dichloromethane were obtained from Merck (Darmstadt, Germany). Polycarbonate membranes (0.45 μm) and 0.22-μm cellulose acetate membranes were obtained from Whatman. All other reagents were of analytical grade or HPLC grade from Merck (Darmstadt, Germany). Benzoic acid as an internal standard was purchased from Sigma-Aldrich. Methanol (high-performance liquid chromatography [HPLC] grade), acetonitrile (HPLC grade), phosphoric acid 85% (analytical grade), sodium dihydrogen phosphate, acetic acid glacial, ammonium acetate, formic acid, ammonium formate, hydrochloride acid, triethylamine, *n*-hexane, and ethyl acetate were purchased from Merck. Double distilled water was used (Ikapharmindo).

2.2. Preparation of VPA-loaded liposomes

VPA-containing liposomes were developed through the thin-film hydration (TFH) technique. Phosphatidylcholine, cholesterol, and VPA were made into five formulas with the comparison ratios shown in Table 1. Phosphatidylcholine and cholesterol dissolved in a 45mL dichloromethane and stirred until a homogeneous solution formed. Furthermore, VPA was dissolved in 5 mL of methanol. A mixture of VPA, phosphatidylcholine, and cholesterol was evaporated using a rotary evaporator at 40 °C. The initial speed of round pumpkin rotation was 50 revolutions per minute (rpm), and then the speed increased by 25 rpm every 30 min to reach 150 rpm. This process was continued until all organic phases evaporated and the film coating formed on the pumpkin wall. The flask was purged with nitrogen gas and allowed to stand for 24 h to ensure the vaporization of the solvent in the liposome. Furthermore, the dried film layer was hydrated with a 50-mL water phase containing phosphate buffer (pH 7.4) using boiling stones (glass beads) to aid peeling. The hydration process was carried out without using vacuum conditions; the temperature used was 40 °C, with an initial speed of 50 rpm, and then increased by 25 rpm every 5 min to 250 rpm. After hydration, this dispersion was allowed to stand for some time for liposome formation. Finally, the multilamellar liposome suspension was bath sonicated for 30 min for size reduction and stored at 4 °C for 24 h. VPA-containing liposomes were separated from the un-entrapped drug with the centrifugation technique at 17,500 rpm for 30 min and washed with buffer twice and used for further study. The size reduction process is carried out using a mini extruder, where the filter membrane is placed in the middle of the extruder. After the mini extruder is assembled on the holder, then the circuit is placed on a heating plate which functions as a temperature regulator for the system during the extrusion process. The extrusion process was carried out by injecting liposomes through a polycarbonate membrane with a pore size of 0.45μm for 8 cycles (non-sterile stage) then re-extruded with a sterile 0.22 μm pore-sized polycarbonate membrane for 5 cycles.

2.3. Characterization of VPA-loaded liposomes

Characterization of VPA entrapment efficiency (EE) and absolute drug loading separated from the liposomes was determined by the downizing sonication method. Then, 0.5 mL of liposome suspension was put into a centrifugation tube with a filter and centrifuged at a for 60 min speed of 3.000 rpm (3K30, Sigma, Germany). VPA that was not encapsulated was separated from the liposome, and it was in the supernatant. The supernatant was again decanted to produce VPA liposome deposits. Methanol (5 mL) was added and sonicated for 5 min to release the VPA compound completely, then diluted up to 100 times. For detection by spectrophotometric methods, samples were centrifuged for 15 min at 7,000rpm. The experiment was repeated three times to ensure the VPA was separated and encapsulated. The amount of drug that was not encapsulated was determined as an over-the-counter drug. VPA compounds in methanol solution were detected at a wavelength of 211 nm. The percentage of drug unentrapped can be calculated from this amount according to the following Eq. (1):

Table 1. Composition, drug EE, and diameter of VPA-loaded liposome.

Liposome Batch No.	Lipid ratio (Drug:Chol:PC)	Size (nm)	Zeta potential. (mV)	Polydispersity index	% EE
Lipo-VPA-1 (F1)	1:10:10	210.1 ± 25.9	−31.87 ± 0.31	0.46 ± 0.05	64.06 ± 3.7
Lipo-VPA-2 (F2)	1:10:25	142.6 ± 1.6	−34.80 ± 0.17	0.18 ± 0.03	70.66 ± 0.81
Lipo-VPA-3 (F3)	1:10:50	139.3 ± 3.00	−42.40 ± 1.06	0.21 ± 0.02	79.06 ± 0.51
Lipo-VPA-4 (F4)	1:10:75	92.01 ± 1.87	−43.47 ± 2.59	0.21 ± 0.01	85.50 ± 1.07
Lipo-VPA-5 (F5)	1:10:90	98.90 ± 1.21	−39.10 ± 0.66	0.23 ± 0.00	83.72 ± 0.54

*PC, phosphatidylcholine; Chol, cholesterol; VPA, valproic acid. Data are mean values ($n = 5$) ± SD.

$$EE\,(\%) = \left(\frac{\text{Total amount of VPA} - \text{Total amount of VPA entrapped}}{\text{Total amount of VPA}}\right) \times 100\% \quad (1)$$

2.4. Determination of size, zeta potential, and polydispersity of VPA-loaded liposomes

VPA-loaded liposomes were observed for particle size using a Malvern zeta sizer (Nano ZS, Malvern instrument, UK) based on the principle of dynamic light scattering. Measurements were made for five formulas on particle size and zeta potential. The samples were diluted and placed in disposable zeta cells. A sample solution with a minimum volume of 0.9 mL was added dropwise into a size cell or a cuvette until the concentration was sufficient; after that, liposome particle was measured. Light scattering was monitored at an angle of 90° and at 25 °C. The analysis was repeated using liposomes, and the significance of the differences was analyzed [20]. All measurements were performed in triplicate.

2.5. Nanoliposome morphology

Observation of the morphology of liposomes were imagine spheric shape and size of the liposome using a TEM (JEOL JEM 1010). A drop liposome by placing 5 μL of the sample in the parafilm liquid specimen. After that, 400 mesh copper grid was prepared for the carbon-coated specimens and left for 10 min to dry. The films were negatively stained with solution for 1 min 0.5% uranyl acetate. Then, it was stirred until a homogeneous solution was formed and then dropped on a copper grid (place of the sample). The filter paper was used to clean the scattered phosphotungstic solution, and the stained samples were characterized at an accelerating voltage of 80 kV and a magnification of 40,000 [21].

2.6. Ex vivo permeation through sheep nasal mucosa

Mucosal surfaces in sheep nasals obtained from slaughter houses (Depok, Indonesia) were used for ex vivo diffusion studies. The tissue is positioned at 45° and liposom formulation is dropped on the mucosa. The mucous membrane used in the penetration test has dimensions of size 0.2 mm × 10 mm × 1.76 cm^2. Phosphate buffered saline is perfused on the mucosa by means of a peristaltic pump with a fixed flow rate with condition pH 7.4, 37 °C. Then, the receptor compartment was filled with system conditions at 37 ± 0.5 °C and stirred at a speed of 300 rpm. After that, the membrane was installed between the receptor compartment and the donor in Franz diffusion cells. A sample of 1 g was applied to the membrane surface with a diffusion area of 1.76 cm^2. Then, the sample was taken as much as 1 mL at time intervals of 15, 30, 60, 120, 180, 240, 300, and 360 min from the receptor compartment using a syringe. After that, the sample was put into a 5-mL measuring flask. Then, the volume was adjusted with PBS (pH 7.4). Samples were measured using HPLC, and the experiment was repeated three times. The results were expressed as the amount of the median substance or percentage diffusion or availability in the brain ex vivo. Transport parameters, e.g., the steady-state flux and the permeability coefficient across the membrane, were calculated according to the steady-state solution of the Fick Eq. (2):

$$J_{ss} = \frac{dM}{dt}\frac{1}{A} = P_e.C \quad (2)$$

where P_e is the permeability diffusion coefficient (cm s^{-1}), C is the initial concentration, J_{SS} is the flux at steady state (mg s^{-1} cm^{-2}), dM is the amount of drug (mg) that can cross the membrane during dt time, and A is the diffusion surface area (cm^2).

The steady-state flux that can pass through the mucous membrane was calculated from the slope value of the line equation obtained by plotting the concentration per unit area against time.

2.7. Comparative pharmacokinetics of VPA in plasma and brain

Prior to the in vivo test, the submission of the method for handling the test animals in this study had obtained permission from the ethics commission at Dr. Hospital. Cipto Mangunkusumo, Faculty of Medicine, University of Indonesia KET-1065/UN2.F1/ETIK/PPM.00.02.2019, with protocol number 19-09-1070. Pharmacokinetic studies were performed on male Wistar rats weighing 250 ± 20 g. The in vivo study was conducted on rat to determine the pharmacokinetic profile. The ethics committee approved the protocol (KET-1065/UN2.F1/ETIK/PPM.00.02.2019). Wistar rats (weight: 250 ± 20 g g, age: 8–10 weeks, n = 6) were maintained in a 12:12-h dark–light cycle at controlled temperature (25 ± 2 °C) and humidity (60 ± 5%), and fed a standard pellet diet for seven days prior to any experimental procedure. Before the actual experiment, all the animals were fasted overnight. The rats were sacrificed with mercy killing at a predetermined post.

The animals in group I (VPA-free drug) and group II (VPA liposomes) were administered 7.5 mg/kg VPA and VPA liposomes body weight by the nasal route. Five rats each were sacrificed at 0, 15, 30, 60, 90, 120, 240, 300, and 360 min, and blood and brain samples were collected for VPA analysis. Around 0.8–1.0 mL of blood was taken using the cardiac puncture method for each time point, and the brain and spinal cord were dissected out, washed twice using normal saline solution, and made free from adhering. The brain tissues were washed three times with saline, cleaned with a soft fabric, weighed, and kept at -40 °C until further investigation. Furthermore, VPA compounds were extracted from brain tissues, homogenized in phosphate buffer pH 7.4, and measured using a spectrophotometry method with HPLC.

2.8. Pharmacokinetic parameters

The following parameters were estimated using the least-squares program of SummitPK (Montrose, CO, USA) to compare VPA levels at various time intervals area under the concentration–time curve from time zero to time t (AUC_{0-t}), terminal elimination half-life ($T_{1/2}$), area under the concentration–time curve from time zero to infinity ($AUC_{0-\infty}$), the maximum plasma drug level (C_{max}), the terminal slope of a semilogarithmic concentration–time curve, and the rate of drug removal from the body (K_{el}).

2.9. Analytical methode high-performance liquid chromatography conditions

VPA compounds that have been extracted in the experiment %EE and %permeation study by Spectrophotometer UV-VIS. The assay was performed on a Waters 2695 series HPLC system equipped with a photodiode array detector (Waters2996). Separation with a mobile phase of acetonitrile–40 mM phosphate buffer (pH 3.5; 44:56 v/v) was performed on a C-8 column (Waters, Symmetry® 5 μm; 150 ′ 3.9 mm2). The analytes were detected using a photodiode array detector at 210 nm wavelength and run at a flow rate of 1 mL/min and a column temperature of 25 °C.

2.10. Sample extraction protocol

Preparation or extraction of VPA from plasma was carried out using the liquid–liquid extraction method. For the liquid–liquid extraction method, the type of acid used is H_3PO_4, while the type of organic phase used is n-hexane. A plasma sample (500 μL) was transferred to a polypropylene tube, and 100 μL of internal standard working solution (1.0 mg/mL), 100 μL of 1 mM phosphoric acid, and 3 mL of n-hexane were added. The mixture was vortex mixed for 2 min and centrifuged at 3000 rpm for 10 min. Then, 2 mL of the organic phase was transferred to the new polypropylene tube, and 250 μL of 0.5% triethylamine was added and vortexed for 2 min. Afterward, the organic phase was discarded, and a 40-μL water phase was injected into the HPLC system. The brain organs are extracted with 4 mL of methanol and vortex until dissolved. Then homogenization was carried out by centrifuging the sample and

transferring the supernatant to a new glass tube which was dried under dry nitrogen flow at 20 psi, 40 °C.

2.11. Statistical analysis

The statistical analysis was performed using SPSS software (version, SPSS Inc. 20.0, Chicago, IL, USA). The statistical analysis was performed using SPSS software (version, SPSS Inc. 20.0, Chicago, IL, USA). T-test was used to compare variables between the two groups. When two or more groups were compared, the analysis of variance was used, followed by a post hoc test. Differences of P 0.05 were considered statistically significant in all tests.

3. Results and discussion

3.1. Determination of size, zeta potential, and polydispersity of VPA-loaded liposomes

In this research, an optimization of the liposome formula was made by comparing the concentration of phospholipids that are shown in Table 1. The liposome formulations were characterized and compared interms of mean particle size, polydispersity index (PdI) and zeta potential. The efficiency test for liposome absorption was conducted in this study [22]. The percentage of VPA absorption is calculated by comparing the measured liposome concentration in liposome deposits after centrifugation with the average concentration of VPA in intact suspension. From the results of the EE test, the highest average percentage of entrants was obtained for F4 (Figure 1). Increasing the concentration of phosphatidylcholine increases the value of EE. The EE value in Formula 5 (1:10:90) is not significantly different from Formula 4 (1:10:75). In previous studies, rivastigmine liposome encapsulation without sonication had a particle size of 10 μm and a release test of 56.0 ± 2.3% with a dialysis bag for 6h [23]. VPA liposomes by sonication with the same method had better drug release values with sonication optimization. Many factors can influence the release of drugs from liposomes, such as solubility in lipids, lipid matrix and concentration, and particle size. The use of liposomes can significantly increase the solubility of lipophilic compounds such as *Allium cepa* [24].

Cholesterol in high concentrations prevent the phospholipids packing and induce orientation and more rigidity to those phospholipids and

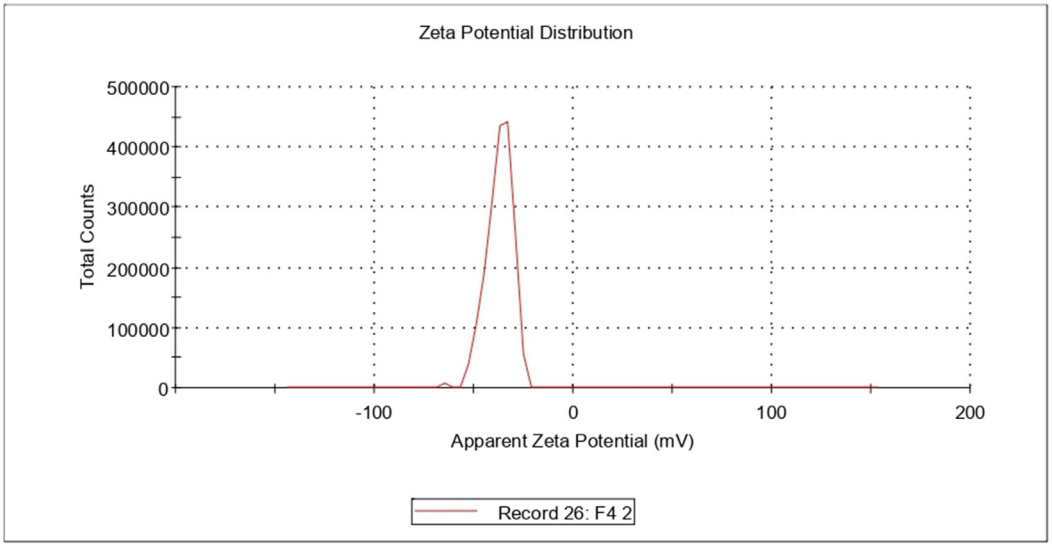

a

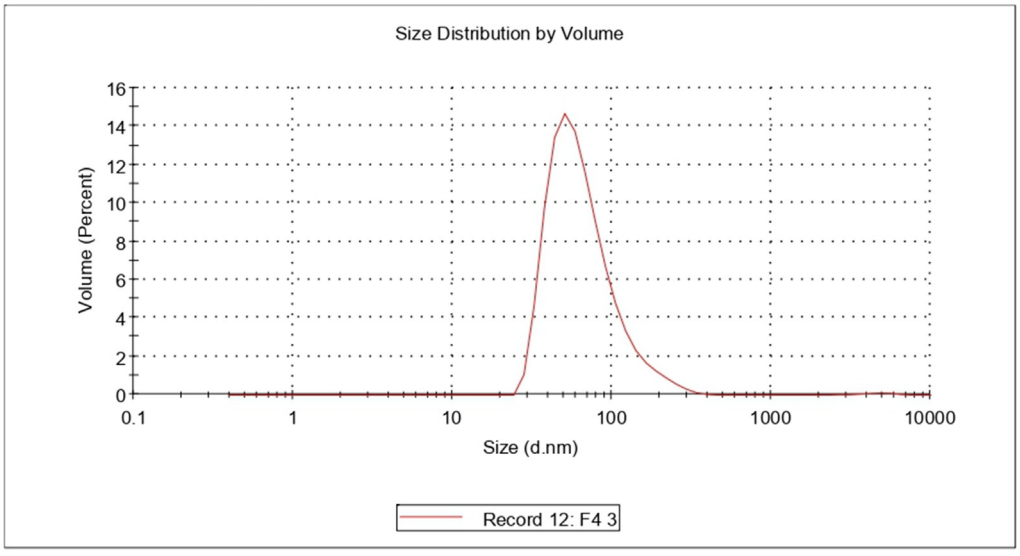

b

Figure 1. Physical properties test using the Zetasizer method on Formula 4 has been optimized (a.) particle size and distribution measurement (nm). (b.) Determination of Zeta potential. (mV).

therefore prevent liposome aggregation [25]. Based on Table 1, the polydispersity index value of liposome samples in the five formulas is based on the volume in the range 0.25–0.50. The low palling PDI value for F4 is 0.28 ± 0.02. The PDI value represents the heterogeneity of the particles [26]. If the PDI value of a sample is less than 0.5, then the sample has a low level of heterogeneity of size and can be said to be a homogeneous sample. phosphatidylcholine distribution based on volume is more representative because it is directly related to the volume of measured particulates [27]. No significant difference was found between the size of the liposomes prepared with phospholipon 90H (Table 1). The presence of different cholesterol did not affect the liposome PDI [23,28,29].

The phosphatidylcholine obtained from the five formulas can be seen in Table 1. The phosphatidylcholine in the five formulas is in the range of 80–250 nm. The measurement values in the five formulas are in the range of the smallest phosphatidylcholine in the F4 formulation, which is 92.01 ± 1.87 nm. Increasing phosphatidylcholine increases particle homogeneity, thereby reducing collisions between particles, resulting in smaller phosphatidylcholine [28, 29, 30]. Therefore, the brown motion of the nanoparticle suspension causes aggregation, the joining of one particle with other particles decreases, and the aggregation of particles decreases [31]. The very phosphatidylcholine of the particles greatly influences the stability of a suspension preparation. The phosphatidylcholine of a nanoparticle sample is also strongly influenced by zeta potential (ZP) as a measure of the magnitude of the electrostatic potential or the repulsion charge between particles in a liposome suspension [28,30].

Zeta potential is a parameter that affects the stability of the dispersion. Zeta can potentially give a picture that the particles in suspension undergo aggregation or flocculation [27]. The measurement results of zeta values of the three liposome formulas can be seen in Table 1. Suspension with a potential zeta value is more positive than +30 mV or more negative than −30 mV [26]. Based on the measurement results, it can be seen that F4 has the best potential zeta value at −43.47 ± 2.59.

Zeta potential is directly related to the distance between particles in a dispersion. The more positive or the more negative the ZP, the more the force repels between particles so that the distance between particles in the dispersion system will be further away. The farther the particle distance, the tendency between particles to aggregate or deflocculate decreases. The results of the absorption efficiency test showed that the average percentage of absorption for the five formulas was 64.06 ± 3.72%, 70.67 ± 0.81%, 79.06 ± 0.51%, 85.50 ± 1.07%, and 83.72 ± 0.54%. These results indicate that the higher the phosphatidylcholine concentration, the higher the percentage of the drug absorbed; the optimal absorption occurs in Formula 4, namely at 85.50 ± 1.07%. The results in Formula 4 are consistent with studies on risperidone liposomes for intranasal preparations. The optimization results of risperidone liposomes are the ratio of cholesterol and SPA (1:8) with a particle size and potential of 91.86 ± 8.42 nm and −53.8 ± 3.90 mV, respectively [32]. The addition of cholesterol causes a decrease in the efficiency of VPA uptake; the higher the amount of cholesterol, the lower the efficiency of VPA. This decrease in absorption efficiency is probably due to the addition of cholesterol, which causes the “salting out” of VPA from the liposome membrane because cholesterol occupies the same position (adsorbed) in the membrane but has a better affinity than VPA. In other studies, the results of the evaluation of zeta potential showed that the addition of cholesterol reduced the zeta potential of the absolute liposome of nimodipine. This is probably due to the inhomogeneous distribution of liposomes and the appearance of cholesterol clots so that the measured zeta potential is a combination of the zeta potential of liposomes and cholesterol particles. Liposomes are pharmaceutical preparations developed in the pharmaceutical world due to their advantages, including increasing the efficacy and therapeutic index and improving drug stability with the encapsulation system. The increase in the concentration of phosphatidylcholine added to the formula results in the higher percentage of drugs that target the CNS [19,30,33,34].

3.2. Morphological characterization

The morphology of liposome can be seen microscopically using TEM, as shown in Figure 2.

This morphological observation was carried out by developing the previously described negative staining method [20,28,29,31]. This method is considered suitable because it does not use heating and uses negative ions from acids to create the color on the background. At the same magnification (40,000×), it is seen that the particles are unilamellar and round in shape [28]. The morphology of VPA liposomes had spherical shapes and a single layer (unilamellar). Formula 4, with a particle size of 92.01 ± 1.87 nm, had homogeneity particles under 200 nm. This result is in accordance with the particle size value in Formula 4 at 92.01 ± 1.87 nm. TEM images also correspond to the homogeneity of the particles.

3.3. Ex vivo permeation behavior of VPA liposomes

In this study, a penetration test of VPA liposomes using Franz diffusion cells was conducted. After a 6-h penetration test with eight sampling points, the amount of VPA cumulated, as shown in Figure 3, from the graph of the cumulative amount of penetrated VPA (ng) per unit area of diffusion area (cm^2), can be calculated as drug flux or call rate (μg cm^{-2} min^{-1}) [35]. Flux was obtained from the slope of the lines in Figure 4 under steady-state conditions following the rule of Fick's law [35].

After a 6-h penetration test with eight sampling points, the cumulative amount of VPA that was penetrated (Figure 3) for the VPA preparation was found. Formulas 4 and 5 showed the highest release values at 6 h, namely 881.85 ± 8.74 and 883, 925 ± 8.76 μg cm^{-2} and are significantly different from the control values, with a value of 378 ± 34.01 μg cm^{-2}. The values of formulas 4 and 5 have been predicted to have high penetration values because their physical properties, such as particle size, zeta potential, and polydispersity index, are better than the other formulas. As the concentration of phosphatidylcholine increases, the speed of drug release increases, and the optimal result is found in Formula 4.

As shown in Figure 4, ex vivo penetration test results indicate that the penetration flux increases in accordance with increased levels of phosphatidylcholine. Formulation VPA:cholesterol:phosphatidylcholine of 1:10:75 (%w/w) also shows the highest value of penetration compared with the other formulas, with a flux value of 200.00 ± 5.61 μg cm^{-2} h^{-1} significantly ($P \leq 0.05$) compared with the control. This proves that the reduction of particles into nanometer size can increase drug penetration through the nasal mucosa. The ability of liposomes to be phospholipid vesicles are biocompatible, flexible, efficient adsorption in the delivery of VPA to the brain. In this case, the increased permeability of valproic acid was obtained with the optimized liposome formulation and the nanometric vesicle size. As a drug delivery system, the amphiphilic nature of liposomes results in the ability of liposomes to contain both hydrophobic and hydrophilic drugs. This mechanism can be achieved by utilizing targeting agent technology on the liposome surface. Also, liposomes based on phosphatidylcholine and cholesterol are flexible that can interact with lipid bilayers and penetrate. This information is expected to carry out further research so that VPA drugs can be projected through intranasal delivery [9,14].

Liposomes are nanoparticle that can increase penetration through the mucous membrane of sheep wells. The penetration of VPA, which is a lipophilic drug, can be enhanced with a nanocarrier. Other researchers have also reported that nanocarriers such as liposomes can increase intranasal penetration [23]. This proves that reducing the particle size to a nanometer size can increase drug penetration through the nasal mucosa. Liposomes, whose main components are phospholipids and cholesterol, can increase drug penetration by various mechanisms. VPA, which is absorbed in liposomes, is in phospholipid layer, which have characteristics similar to the lipid bilayer in the stratum corneum. This is by the theory of the effect of liposomes, which can increase drug

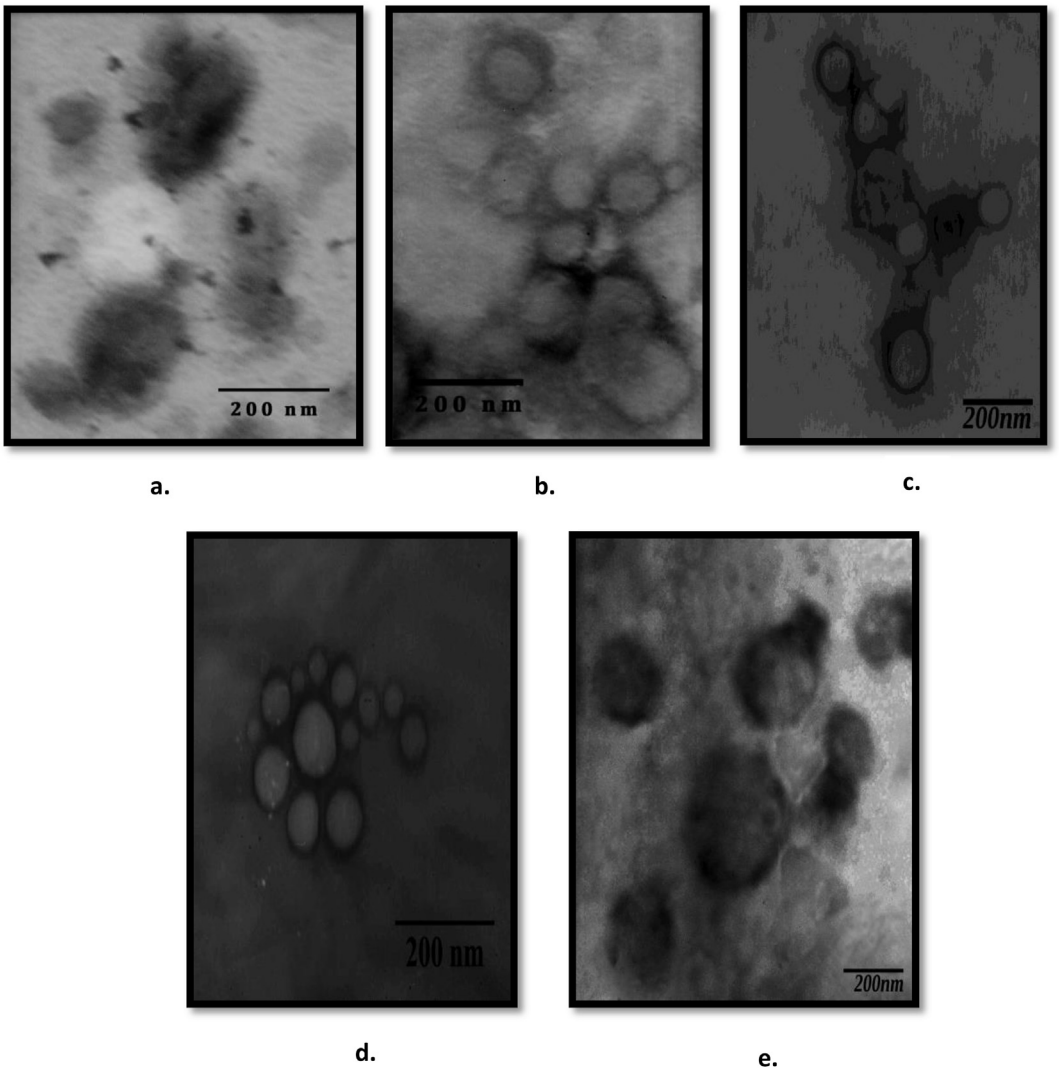

Figure 2. Particle size distribution of VPA liposomes by TEM. (a) Formula 1, (b) Formula 2, (c) Formula 3, (d) Formula 4, and (e) Formula 5.

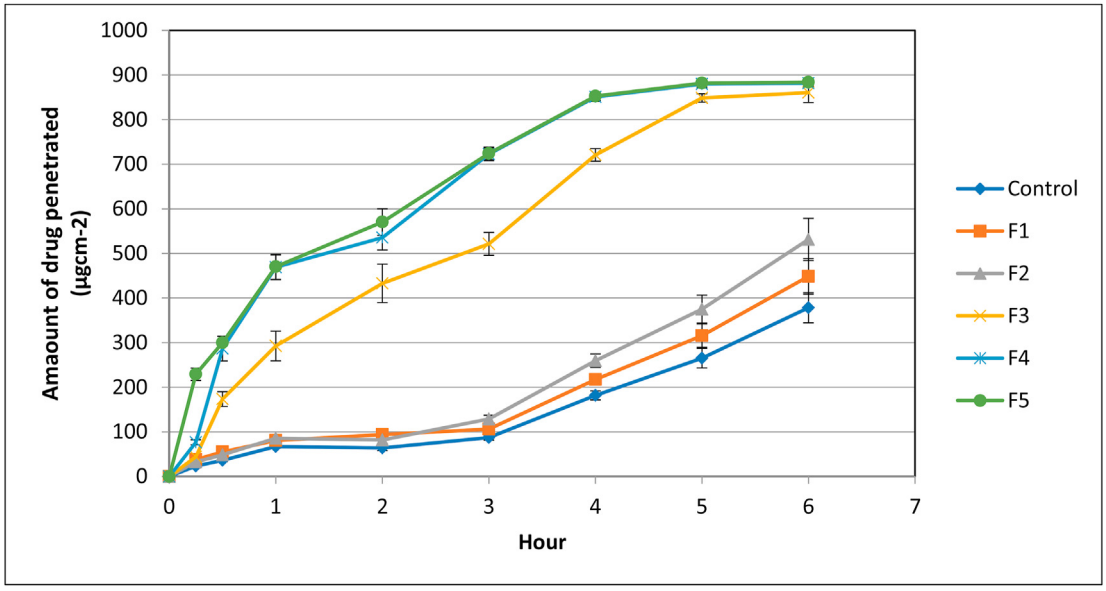

Figure 3. The VPA permeation profile of the liposome formula in F1, F2, F3, F4, and F5 was measured for 6 h and was measured by spectrophotometric method and presented in terms of cumulative drug release percentage (mean ± standard deviation,$n = 3$).

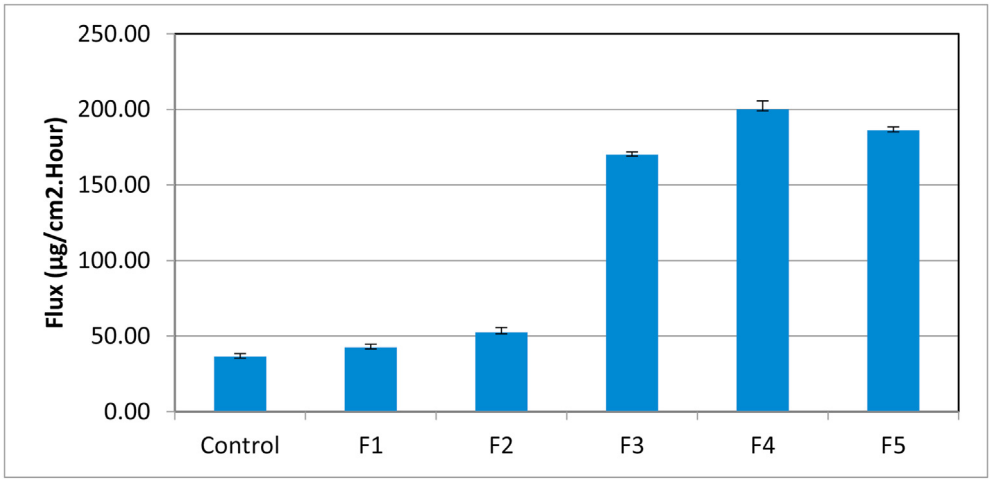

Figure 4. Flux profile at F1, F2, F3, F4, and F5 describes the level (Flux (µg/cm2.Hour) can penetrate through the mucous membranes of the sheep's nose (mean ± standard deviation, n = 3).

penetration through the mucosa because phospholipids that absorb VPA have a suitable partition coefficient to penetrate. The higher the partition coefficient, the easier it is for material to penetrate through the stratum corneum [22].

3.4. Comparative pharmacokinetics of VPA in plasma and brain

The results of the in vivo test on mice by comparing the bioavailability of VPA in blood plasma and brain are shown in Figure 5. This method has previously been validated analytical HPLC method. The study was conducted to test and compare valproic acid concentration in the blood and brain. In addition, it was conducted to compare valproic acid liposomes and free drugs administered intranasally. The dose chosen in this study refers to previous data on particle physical characterization data, in vitro penetration, and ex vivo release, namely formulation 4.

As shown in Figure 5, the graph on rat blood plasma in less than 15 min, the control group showed higher penetration than the liposome group. The value of C_{max} in the control group was 6.49 ± 0.79 g mL^{-1} and decreased at the next time point. Meanwhile, for more than 30 min, the penetration of the liposome group was higher than that of the control group. The value of C_{max} in the liposome group was 12.72 ± 0.91 µg mL^{-1} at 90 min and decreased at the next time point.

Based on Table 2, it can be seen that the maximum concentration (C_{max}) was highest in Lipo-VPA (F4), which was 12.72 g mL^{-1} at the maximum time value (t_{max}) at 90 min. The VPA liposome group gave the control group a C_{max} value of 6.49 ± 0.79 g mL^{-1} and the maximum time value (t_{max}) at 30.00 min. The values of AUC_{0-t}, $AUC_{t-\infty}$, and $AUC_{0-\infty}$ showed that VPA liposomes had significantly different values in the control treatment group. Based on the statistical comparison of the liposome group and the control group, the *t*-test showed a significant difference ($P < 0.05$).

The concentration of VPA in the brain following oral and nasal administration showed the same pattern as observed in the case of plasma, suggesting a better bioavailability of the drug following nasal delivery (Figure 6). As shown in Figure 6, the graph on the brains of rats in less than 15 min, the control group gave higher penetration than the liposome group. The value of C_{max} in the control group was 6.54 g mL^{-1} and decreased at the next time point. Meanwhile, at 90 min later, liposome penetration was higher than in the control group. The value of C_{max} in the liposome group was 18.06 g mL^{-1} and decreased at the next time point.

From Table 3, it can be seen that the maximum concentration (C_{max}) was highest in the Lipo-VPA (F4) group, which was 18.06 ± 1.64 µg $^{-1}$ at the maximum time value (t_{max}) at 90 min. The VPA liposome group

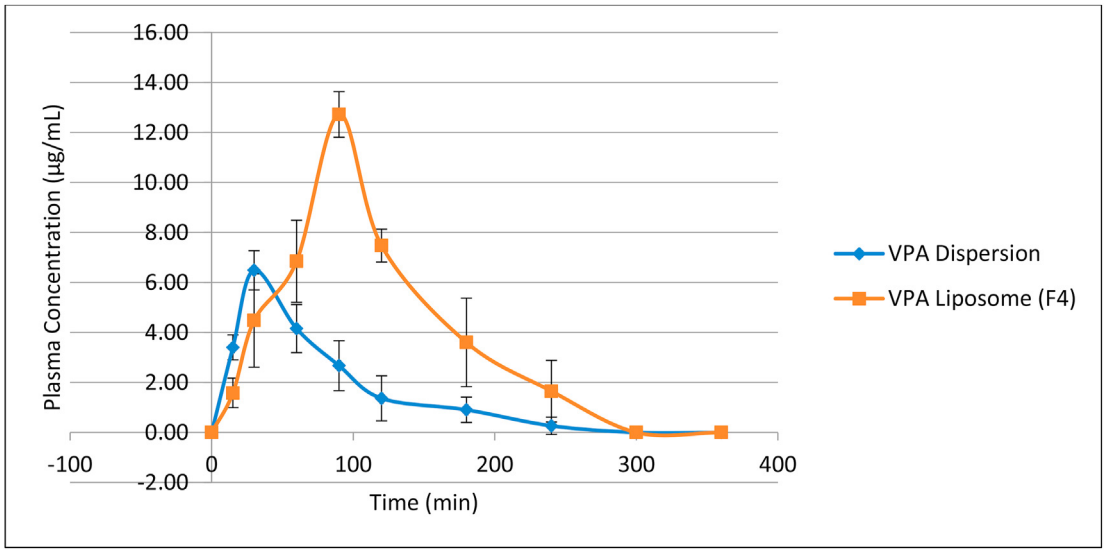

Figure 5. Mean plasma concentration and time profile of VPA with various routes of administration (mean ± standard deviation, $n = 5$).

Table 2. Pharmacokinetic parameters of VPA in plasma after various routes of administration (mean ± SD, $n = 5$).

Pharmacokinetic parameters	Plasma free drug	±SD	Plasma liposome (F4)	±SD	Liposome/free drug
C_{max} (μg mL^{-1})	6.49	0.79	12.72*	0.91	1.961
t_{max} (min)	30.00	0.00	90.00*	0.00	3.000
AUC_{0-t} (μg min mL^{-1})	511.22	122.10	1449.88*	154.30	2.836
$AUC_{0-\infty}$ (μg min mL^{-1})	589.81	171.99	1631.11*	254.97	2.765
$t_{½}$ (min)	71.48	22.81	57.17*	32.03	0.800
K_{el} (min)	0.011	0.00	0.015	0.01	1.364

Note: $P < 0.05$, compared with free drug intranasal.
Abbreviations: VPA, valproic acid; SD, standard deviation; AUC_{0-t}, area under the concentration–time curve from time zero to time t; $AUC_{0-\infty}$, area under the concentration–time curve from time zero to infinity; $t_{1/2}$, terminal elimination half-life; C_{max}, maximum plasma drug level; K_{el}, rate of drug removal from the body.

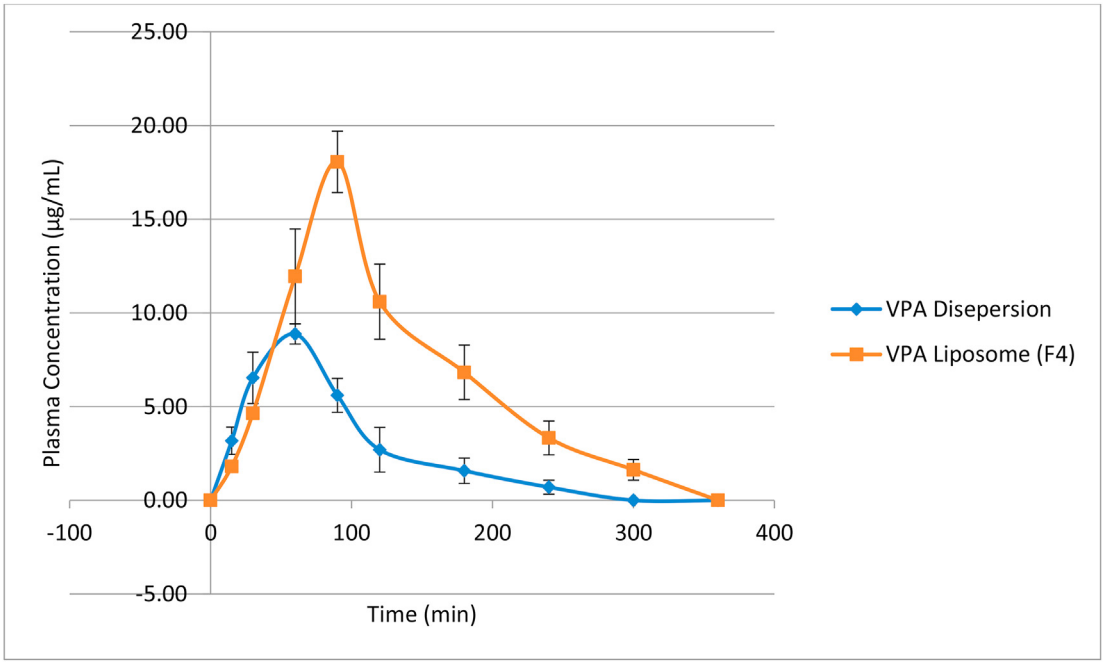

Figure 6. Mean brain concentration and time profile of VPA with various routes of administration (mean ± standard deviation, $n = 5$).

Table 3. Pharmacokinetic parameters of VPA in the brain after nasal routes of administration (mean ± SD, $n = 6$).

Parameter	Free drug	SD	Lipo-VPA (F4)	SD	Liposome/free drug
C_{max} (μg mL^{-1})	8,87	0,54	18,06	1,64	2,036
t_{max} (min)	60,00	0,00	90,00	0,00	1,500
AUC_{0-t} (μg min mL^{-1})	872,43	135,38	2256,69	104,10	2,587
$AUC_{0-\infty}$ (μg min mL^{-1})	944,02	201,87	2428,56	147,99	2,573
$t_{½}$ (min)	60,28	32,39	67,11	27,21	1,113
K_{el}	0,013	0,00	0,012	0,00	0,923

Note: $P < 0.05$, compared with free drug intranasal.
Abbreviations: VPA, valproic acid; SD, standard deviation; AUC_{0-t}, area under the concentration–time curve from time zero to time t; $AUC_{0-\infty}$, area under the concentration–time curve from time zero to infinity; $t_{1/2}$, terminal elimination half-life; C_{max}, maximum brain drug level; K_{el}, rate of drug removal from the body.

showed the maximum concentration (C_{max}) value compared with the control group, with a value of 8.87 ± 1.98 μg $^{-1}$ and the maximum time value (t_{max}) at 60.00 min. The values of AUC_{0-t}, $AUC_{t-\infty}$, and $AUC_{0-\infty}$ showed that VPA liposomes had significantly different values from the control treatment group. Based on the statistical comparison of the liposome group and the control group, the *t*-test showed a significant difference ($P < 0.05$).

Complete data on the results of the comparison of the *t*-test are given in the Appendix. Intranasal administration increases drug biodistribution to the brain [36]. The increase in AUC and mean residence time (MRT) hows that more drug absorption into the brain via intranasal liposomal encapsulation can increase extended release and retention of drugs in the brain for a longer time [37]. The difference in C_{max} and $AUC_{0-\infty}$ values after administration of the solution without intranasal encapsulation and formulation into liposomes was found to be significant [32].

Liposome optimization by reducing particle size also showed a significant increase in the $AUC_{0-\infty}$ data for liposomes showing increased permeation through the BBB and distribution to the brain [38]. Liposome encapsulation showed an increase in the residence time of the drug in the brain, which showed a significant increase in the elimination half-life in

the brain. Moreover, the MRT value of liposomes of loaded VPA increased considerably compared with the pure drug. The amount of VPA for encapsulation was statistically significant in brain tissue ($P < 0.05$) compared with the VPA solution. Therefore, it was concluded that liposomes loaded with VPA increased the rate of drug absorption into the brain compared with pure drugs. Lipophilicity, molecular mass, route of administration, and release of P-glycoprotein are factors considered to determine drug transfer across the BBB [39].

This study is also in agreement with the factors mentioned above, as the liposome formulation achieves better absorption into the brain after intranasal administration compared with over-the-counter drugs. This is also because the route of drug administration from the nasal mucosa has a direct channel to the brain [40]. The intranasal route is a promising pathway for drug delivery into the CNS [41].

4. Conclusion

Valproic acid liposome formula selected was formula 4 with spherical morphology, the highest percentage of an adsorbed drug, polydispersity index, and has zeta potential. The ex vivo penetration test and penetration flux of valproic acid from the liposome preparation were higher with the valproic acid control solution. Intranasal administration of valproic acid can increase the bioavailability of valproic acid levels in the brain compared to blood plasma. Attempts at encapsulation of liposomes by intranasal delivery allow higher valproic acid to cross the blood-brain level. The liposome method, which has sustainable properties, is also appropriate for improving patient compliance. Intranasal administration is effective in rapid delivery to the brain, avoiding first-pass metabolism in the liver, eliminating the need for system delivery, and reducing unwanted system side effects. Furthermore, as it persists, this method allows easy and direct self-administration to the patient and can reduce administration.

Declarations

Author contribution statement

Alhara Yuwanda: Conceived and designed the experiments; Analyzed and interpreted the data; Contributed reagents, materials, analysis tools or data; Wrote the paper.

Silvia Surini: Analyzed and interpreted the data; Wrote the paper.

Yahdiana Harahap:Contributed reagents, materials, analysis tools or data.

Mahdi Jufri: Conceived and designed the experiments; Performed the experiments; Analyzed and interpreted the data; Wrote the paper.

Funding statement

This work was supported by Directorate of Research and Comunity Engagements Universitas Indonesia No: NKB-0200/UN2. R3.1/HKP.05.00/2019 for a research Grant of the University's Base Research Program.

Data availability statement

Data included in article/supplementary material/referenced in article.

Declaration of interests statement

The authors declare no conflict of interest.

Additional information

Supplementary content related to this article has been published online at https://doi.org/10.1016/j.heliyon.2022.e09030.

References

[1] M. Kapoor, J.C. Cloyd, R.A.N.U. Siegel, J Control Release, 2016 [Internet].
[2] R.J.Y. Ho, J. Chien, Trends in translational medicine and drug targeting and delivery: new insights on an old concept - targeted drug delivery with antibody-drug conjugates for cancers, J. Pharmaceut. Sci. 103 (1) (2014) 71–77.
[3] S. Grassin-delyle, A. Buenestado, E. Naline, C. Faisy, S. Blouquit-laye, L. Couderc, et al., Pharmacology & Therapeutics Intranasal drug delivery : an ef fi cient and non-invasive route for systemic administration Focus on opioids, Pharmacol. Ther. 134 (3) (2012) 366–379.
[4] L. Sherwood, Human Physiology from Cells to Systems Ninth Edition, Appetite, 2016.
[5] D.U. Silverthorn, B.R. Johnson, W.C. Ober, C.W. Garrison, A.C. Silverthorn, Human Physiology an Integrated Approach Edition 6E, Pearson Education Inc., 2013.
[6] J.T. DiPiro, R.L. Talbert, G.C. Yee, G.R. Matzke, B.G. Wells, L.M. Posey, et al., Book Review: Pharmacotherapy: A Pathophysiologic Approach, seventh ed., Ann Pharmacother, 2009.
[7] NM, SG, SN, BS, SP, SP, Nasal drug delivery: problem solution and its application, J. Curr. Pharma. Res. 4 (3) (2014) 1231–1245.
[8] A. Pires, A. Fortuna, G. Alves, A. Falcão, Intranasal Drug Delivery : How , Why and what for ? 12, 2009, pp. 288–311 (3).
[9] A.D. Stock, S. Gelb, O. Pasternak, A. Ben-Zvi, C. Putterman, The blood brain barrier and neuropsychiatric lupus: new perspectives in light of advances in understanding the neuroimmune interface, Autoimmun. Rev. 16 (6) (2017) 612–619.
[10] P.C. Pires, A.O. Santos, Nanosystems in nose-to-brain drug delivery : a review of non-clinical brain targeting studies, J. Contr. Release 270 (September 2017) (2018) 89–100.
[11] J. Rohrer, N. Lupo, A. Bernkop-Schnürch, Advanced formulations for intranasal delivery of biologics, Int. J. Pharm. 553 (1–2) (2018) 8–20.
[12] N. Ishizue, S. Niwano, M. Saito, H. Fukaya, H. Nakamura, T. Igarashi, et al., Polytherapy with Sodium Channel-Blocking Antiepileptic Drugs Is Associated with Arrhythmogenic ST-T Abnormality in Patients with Epilepsy 40, Seizure, 2016, pp. 81–87 [Internet].
[13] J.L. Scism, K.M. Powers, A.A. Artru, L. Lewis, D.D. Shen, Probenecid-inhibitable Efflux Transport of Valproic Acid in the Brain Parenchymal Cells of Rabbits : a Microdialysis Study 884, 2000, pp. 77–86.
[14] S. Eskandari, J. Varshosaz, M. Minaiyan, M. Tabbakhian, Brain delivery of valproic acid via intranasal administration of nanostructured lipid carriers: in vivo pharmacodynamic studies using rat electroshock model, Int. J. Nanomed. (2011).
[15] H. Wang, Q. Huang, H. Chang, J. Xiao, Y. Cheng, Stimuli-responsive dendrimers in drug delivery, Biomater. Sci. 4 (3) (2016) 375–390.
[16] T. Lopez, Biocompatible Titania Microtubes Formed by Nanoparticles and its Application in the Drug Delivery of Valproic Acid 29, 2006, pp. 70–74.
[17] S.F. Tan, B.P. Kirby, J. Stanslas, H Bin Basri, Characterisation, in-vitro and in-vivo evaluation of valproic acid-loaded nanoemulsion for improved brain bioavailability, J. Pharm. Pharmacol. (2017).
[18] N. Mori, S ichi Ohta, Comparison of anticonvulsant effects of valproic acid entrapped in positively and negatively charged liposomes in amygdaloid-kindled rats, Brain Res. 593 (2) (1992) 329–331.
[19] T.M. Allen, P.R. Cullis, Liposomal drug delivery systems: from concept to clinical applications, Adv. Drug Deliv. Rev. (2013).
[20] M. Çağdaş, A.D. Sezer, S. Bucak, Liposomes as potential drug carrier systems for drug delivery, in: Application of Nanotechnology in Drug Delivery, 2014.
[21] Y. Zhang, M. Huo, J. Zhou, A. Zou, W. Li, C. Yao, et al., DDSolver: an add-in program for modeling and comparison of drug dissolution profiles, AAPS J. 12 (3) (2010) 263–271.
[22] S.P. Acharya, K. Pundarikakshudu, P. Upadhyay, P. Shelat, A. Lalwani, Development of phenytoin intranasal microemulsion for treatment of epilepsy, J. Pharm. Investig. 45 (4) (2015) 375–384.
[23] K. Arumugam, G.S. Subramanian, S.R. Mallayasamy, R.K. Averineni, M.S. Reddy, N. Udupa, A Study of Rivastigmine Liposomes for Delivery into the Brain through Intranasal Route 58, 2008, pp. 287–297.
[24] V. Singh, P. Krishan, R. Shri, Amelioration of ischaemia reperfusion-induced cerebral injury in mice by liposomes containing Allium cepa fraction administered intranasally. Artif Cells, Nanomed. Biotechnol. (2018).
[25] R.C. Rowe, P.J. Sheskey, M.E. Quinn, Handbook of Pharmaceutical Excipients, sixth ed., Handbook of Pharmaceutical Excipients, 2009. - (Malestrom).
[26] P.A. Carson, C.J. Mumford, Hazardous chemicals handbook, Hazard Chem. Handb. (2013) 1–378.
[27] Malvern Instruments Ltd, A basic guide to particle characterization, Inf. White Pap. (2012).
[28] N. Monteiro, A. Martins, R.L. Reis, N.M. Neves, Liposomes in tissue engineering and regenerative medicine, J. R. Soc. Interface (2014).
[29] R. Raj, P.M. Raj, A. Ram, Lipid based noninvasive vesicular formulation of cytarabine: nanodeformable liposomes, Eur. J. Pharmaceut. Sci. (2016).
[30] S. Cunha, M.H. Amaral, J.M. Sousa Lobo, A.C. Silva, Lipid nanoparticles for nasal/intranasal drug delivery, Crit. Rev. Ther. Drug Carrier Syst. 34 (3) (2017) 257–282.
[31] A. Chonkar, U. Nayak, N. Udupa, Smart Polymers in Nasal Drug Delivery, Indian Journal of Pharmaceutical Sciences, 2015.
[32] R. Narayan, M. Singh, O. Ranjan, Y. Nayak, S. Garg, Development of risperidone liposomes for brain targeting through intranasal route, Life Sci. 163 (2016) 38–45. Available from:.
[33] A.V. Vaidya, U.A. Shinde, H.H. Shimpi, Preliminary studies on brain targeting of intranasal atomoxetine liposomes, Int. J. Pharm. Pharmaceut. Sci. (2016).
[34] Y. Chen, L. Liu, Modern methods for delivery of drugs across the blood-brain barrier, Adv. Drug Deliv. Rev. (2012).

[35] H. Malinowski, P. Marroum, V.R. Uppoor, W. Gillespie, H.Y. Ahn, P. Lockwood, et al., FDA guidance for industry extended release solid oral dosage forms: development, evaluation, and application of in vitro/in vivo correlations, Dissolution Technol. (1997).
[36] N. Ahmad, R. Ahmad, M.A. Alam, F.J. Ahmad, Quantification and brain targeting of eugenol-loaded surface modified nanoparticles through intranasal route in the treatment of cerebral Ischemia, Drug Res. 68 (10) (2018) 584–595.
[37] Li Z. Ling, Peng S. Feng, X. Chen, Zhu Y. Qing, Zou L. Qiang, W. Liu, et al., Pluronics modified liposomes for curcumin encapsulation: sustained release, stability and bioaccessibility, Food Res. Int. 108 (2018) 246–253.
[38] J. Wang, Y. Wei, Y.R. Fei, L. Fang, H.S. Zheng, C.F. Mu, et al., Preparation of mixed monoterpenes edge activated PEGylated transfersomes to improve the in vivo transdermal delivery efficiency of sinomenine hydrochloride, Int. J. Pharm. 533 (1) (2017) 266–274.
[39] P. Mura, N. Mennini, C. Nativi, B. Richichi, In situ mucoadhesive-thermosensitive liposomal gel as a novel vehicle for nasal extended delivery of opiorphin, Eur. J. Pharm. Biopharm. 122 (2018) 54–61.
[40] L. Salade, N. Wauthoz, J. Goole, K. Amighi, How to characterize a nasal product. The state of the art of in vitro and ex vivo specific methods, Int. J. Pharm. 561 (January) (2019) 47–65. Available from:.
[41] C. Caddeo, L. Pucci, M. Gabriele, C. Carbone, X. Fernàndez-Busquets, D. Valenti, et al., Stability, biocompatibility and antioxidant activity of PEG-modified liposomes containing resveratrol, Int. J. Pharm. 538 (1–2) (2018) 40–47.